Mathematical analysis of the Real Time Array PCR (RTA PCR) process

J. Frits Dijksman [a,b] **, Anke Pierik** [a]

[a] Philips Research Europe, High Tech Campus 11, 5656AE Eindhoven, The Netherlands.
[b] Present affiliation: University of Twente, Physics of Fluids Department, Drienerlolaan 5, 7522 NB Enschede, The Netherlands.
Corresponding author: J.Frits Dijksman,
University of Twente, Physics of Fluids Department, Drienerlolaan 5, 7522 NB Enschede,
The Netherlands.
Telephone: +31 6 2334 1331. E-mail: j.f.dijksman@ziggo.nl

Abstract

Real Time Array PCR (RTA PCR) is a recently developed biochemical technique that measures amplification curves (like with quantitative real time Polymerase Chain Reaction (qRT PCR)) of a multitude of different templates in a sample.
It combines two different methods in order to profit from the advantages of both, namely qRT PCR (real time quantitative detection) with microarrays (high multiplex capability). This enables the quantitative detection of many more target sequences than can be done by qRT PCR. Thereby, the concentration of many different target molecules originally present in a sample can be measured. Labelled primers are used that are first elongated to form labelled amplicons in the bulk and these can hybridize to capture probes immobilized on the surface of the microarray. During each PCR cycle, there is a time window available during which the formed labelled amplicons can hybridize to the target sequences (capture probes) on the microarray surface. By detection of the fluorescence of the spots on the microarray, amplification curves comparable to qRT PCR are obtained, which can be used to deduce the information needed on the presence and the amount of targets originally present in the sample.
We present a mathematical model that provides fundamental insights in the different steps of Real Time Array PCR (RTA PCR). These findings can be used to optimize the different biochemical processes taking place.
At the microarray surface specific molecules are captured and taken away from the solution, causing a concentration gradient that powers a material flow towards the microarray surface. Only labelled strands of the amplicons are captured by probes on the microarray surface and as a result locally the PCR process is not symmetric anymore. Moreover, in course of the process more and more single stranded DNA renatures, leaving relatively less strands and complexes available for hybridization.
The main conclusion is that surface fluorescence scales with the bulk concentration of the targets involved. Our analysis shows that the C_t value is only slightly dependent on the initial enzyme load and the degradation of the capture probes. The C_t value, however, does depend strongly on the rate constants of the annealing/hybridization reactions in the bulk and on surface. Local asymmetry appears to be a minor effect.

Keywords:

Polymerase Chain Reaction, Diffusion, Hybridization, Microarray, DNA, Molecular Diagnostics.

1 Introduction

Real Time Array PCR (RTA PCR) is a recently developed biochemical technique to measure real time amplification curves of a multiple of different templates in a PCR sample (**Remacle et al., 2006; Remacle et al., 2007; Khodakov et al., 2008; Pierik et al., 2011**). It combines the real time access to process data as provided by Real Time PCR (qRT PCR) and thereby quantitative information on the initial number of target molecules present in the sample and the high multiplex capability of a microarray based assay. In qRT PCR TaqMan probes, molecular beacons or intercalating dyes are used that become fluorescent in the course of the amplification reaction. The detected fluorescence increase in the bulk is a direct measure for the amount of amplified templates. To quantify the fluorescence increase, the cycle threshold value (C_t-value) is used, defined as the cycle number during which the signal has increased above the background value. The larger the value of C_t of a certain constituent, the lower its expression (initial concentration). For array based methods often fluorescently labelled amplicons are being detected, which are formed during amplification by elongation of a labelled primer.

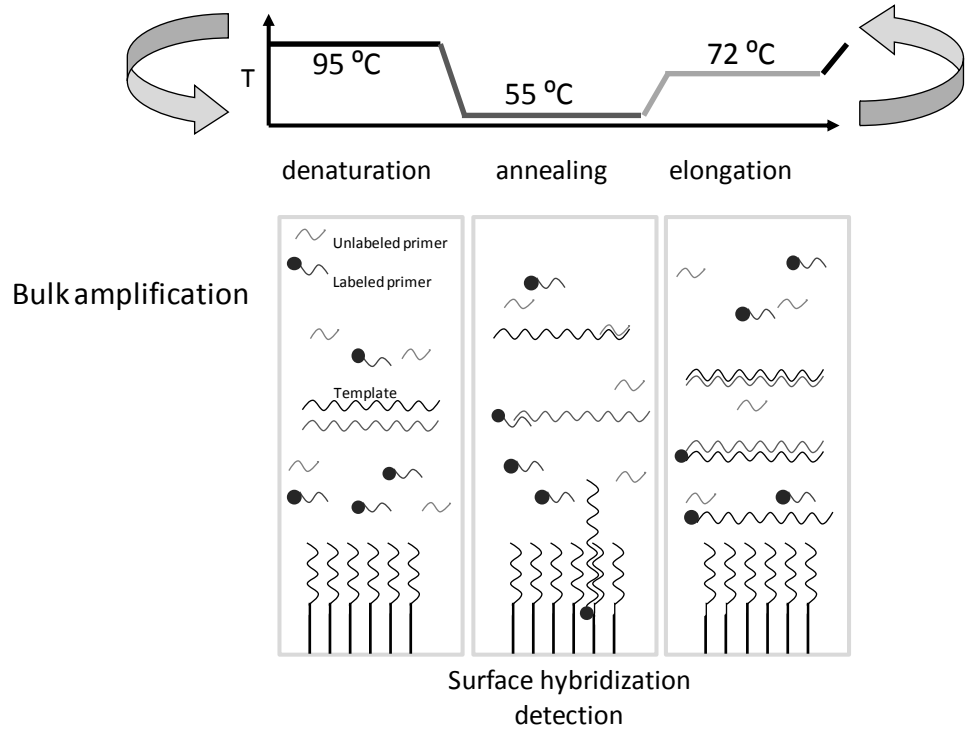

Figure 1 Concept of Real Time Array PCR (RTA PCR). During annealing in course of time labelled amplicons hybridize with capture probes immobilized on the array surface. Fluorescent molecules are indicated by black dots.

Figure 1 outlines the concept of RTA PCR. In the bulk, like in normal qRT PCR, a three-step amplification reaction is running. On the microarray surface, a different process namely surface hybridization, takes place in parallel.
During the high temperature step, all double stranded DNA is denatured. Subsequently during the annealing phase, next to bulk reactions like formation of binary complexes of primers and amplicons on the one hand and the formation of tertiary complexes involving the enzymes and the binary complexes followed by elongation on the other hand, labelled amplicons hybridize to the microarray surface. At the end of the annealing step, the surface fluorescence is measured. After annealing the temperature is raised and the elongation that already started slowly during annealing, increases in rate. All binary and surface complexes most probably will melt, only tertiary complexes will survive. After the elongation phase the temperature is raised again and all double stranded DNA falls apart into single stranded DNA. This process is repeatedly done during a number of consecutive PCR cycles. Per cycle the concentration of amplicons increases and more and more labelled amplicons (targets) are captured by specific probes immobilized in spots of the microarray. After each anneal/ hybridization period the fluorescent spot pattern is scanned. In this way the dynamics of the Real Time Array PCR process are followed real time. Real time amplification curves of all spots can be created by plotting the fluorescence of each individual spot as a function of the PCR cycle number.

From a biochemical process technology point of view, there are specific differences between the Real Time PCR (qRT PCR) process and the Real Time Array PCR (RTA PCR) process.
Real Time PCR is a bulk process, since everywhere the same process is running under the same conditions. Real Time PCR is a symmetric process, provided the mix starts with equal amounts of reverse and forward primers. Furthermore, qRT PCR is a transient process. The timing of the different steps must be chosen such that at the end of each step a steady state is reached. This means that during annealing all amplicons have reacted with primers to form secondary complexes and subsequently tertiary complexes with enzymes, that all primers have been elongated and that during denaturation all double stranded DNA has been decomposed into single stranded DNA. Real Time Array PCR is not only a bulk process, because at the microarray surface specific molecules are captured and taken away from the solution, causing a concentration gradient that powers a material flow towards the microarray surface. This concentration gradient develops over time.

Since the capture probes are only complementary to and hybridize with the labelled strands of the amplicons, the unlabelled strands will be available in larger concentrations close to the microarray surface leading to an asymmetry in the concentration of sense and antisense strands at that location.

Finally, because of the surface reaction, another time constant has entered the scene, namely the time it takes before the surface concentration has reached a steady state that will allow for a precise detection of the surface fluorescence.

1.1 Description of set-up

For modelling the reactions taking place, experimentally related parameters need to be given. These are derived from typical experimental data (**Pierik et al, 2011**).
Usually, a RTA PCR is carried out in a differently shaped reaction chamber than a standard PCR well, since one of the surfaces needs to contain a flat microarray. In order to have comparable volumes, a disk shaped reaction chamber that measures 5.5 mm across and has a height of 1 mm can, for example, be considered. Its volume equals 25 µl ($25*10^{-9}$ m^3), with one of the flat faces of the reaction chamber carrying the microarray pattern. The material used for making the cartridge containing the reaction chamber is typically glass, since most of the microarray slides are made of glass. Capture oligonucleotides are dissolved to concentrations of $3*10^{-3}$ mol/m^3 and are ink jet printed in square or hexagonal patterns. The wet volume (usually 1 nl) dries to a spot of around 200 µm diameter. Such a spot contains $1.8*10^9$ probes, having a surface density of probes equal to $5.75*10^4$ probes/μm^2. The probes are fixed to the microarray surface by UV exposure. It should be mentioned that not all printed capture probes are immobilised and will be washed away leaving a somewhat lower surface density behind (**Pierik et al., 2008**).

A typical process that we use as a starting point for the mathematical experiments runs as follows. The content of the reaction chamber is subjected to temperature cycling: during 10 minutes a hot start at 95 °C, followed by 60 cycles of 120 seconds at 55 °C (annealing and hybridization), 40 seconds at 72 °C (elongation) and 20 seconds at 95 °C (denaturation or melting). During the last 20 seconds of the annealing step the fluorescent pattern of the microarray is scanned.

Apart from the degradation of the activity of enzymes in the bulk due to thermal cycling (**Sambrook and Russell, 2001**), adsorption of enzymes or other reaction components to the wall of the glass reaction chamber of the Real Time Array PCR set-up may be a point of concern. Proteins and enzymes generally adsorb onto glass surfaces (**Erill et al, 2003; Potrich et al, 2010**). The material used for qRT PCR vials is usually a biocompatible and inert polymer, which is optimized to have a low interaction with proteins and enzymes. The shape of the vial is such that the surface area per unit volume is small; the flat reaction chamber of the Real Time Array PCR cartridge is in that respect less favourable. Though BSA is added to reduce surface adsorption, it may not prevent fully that part of the reaction components and especially the enzymes adsorb onto the glass surface.

The scope of the present paper is as follows. We start with setting up a concise theoretical framework for the qRT PCR process, because the outcomes of this analysis will act as initial and boundary conditions for the hybridization process at the microarray surface. We continue with analysing the hybridization kinetics at the microarray surface and the consequences of the surface hybridization on the concentration gradients in the fluid above the microarray surface. Here we will assume that only single stranded DNA can hybridize. This despite the fact that the primer sites and the capturing site on the amplicon are in general non-overlapping. But the

tertiary complex of a single stranded DNA with a primer and enzyme is to a large extent sterically hindered, meaning that hybridization with a capture probe immobilized at the array surface will be most unlikely.

1.2 Nomenclature

a: radius semi-spherical dome [m]
b: radius spot [m]
C_t: cycle number at which fluorescence is above threshold [-]
c^*: dimensionless concentration [-]
c: molar concentration [mol/m^3]
$c_{template}$: initial concentration of templates at the start of the PCR process [mol/m^3]
c_0: initial concentration at the start of the annealing/hybridization phase [mol/m^3]
$c_A(t)$: molar concentration species A (labeled sense ssDNA) [mol/m^3]
$c_B(t)$: molar concentration species B (unlabeled antisense ssDNA) [mol/m^3]
c_{TAQ}: initial concentration Taq polymerase [mol/m^3]
c_{dNTP} : concentration dNTP's during process [mol/m^3] (for each dNTP's : assuming equal consumption of dATP, dCTP, dGTP and dTTP, total concentration of triphosphates 4 c_{dNTP}).
c_{dNTP0} : initial concentration dNTP's [mol/m^3] (for each dNTP's : dATP, dCTP, dGTP and dTTP, total concentration of triphosphates 4 c_{dNTP0}), typically our protocol uses 0.2 mol/m^3 per dNTP.
$c_{dNTP}(n)$: concentration of dNTP's needed to elongate all available tertiary complexes [mol/m^3]
c_{p0}: initial concentration at the start of the PCR process of forward and reverse primers [mol/m^3] (total initial concentration primers $2c_{p0}$, typically c_{p0}=0.3*10^{-3} mol/m^3)
c_{pF}: concentration forward primers during annealing [mol/m^3]
c_{pR}: concentration reverse primers during annealing [mol/m^3], typically $c_{pF} = c_{pR}$
$\mathcal{D}$: diffusion coefficient [m^2/s]
E: PCR efficiency
$E_{elongation}$: elongation factor
f_{TAQ}: fraction reduction of active enzyme per cycle [-]
f_{probes}: fraction reduction of active probes on the microarray per cycle [-]
h, h': coefficients used for the radiation transfer coefficient [1/m]
K_m: Michaelis-Menten constant for elongation reaction [mol/m^3]
k: annealing rate constant for formation of binary complexes of ssDNA with primers [m^3/s/mol]
k_{ass}: association rate constant Langmuir surface reaction [m^3/s/mol]
k_{diss}: dissociation rate constant Langmuir surface reaction [1/s]
k_{dsDNA}: annealing rate constant for formation of dsDNA [m^3/s/mol]
L: number of bases in amplicons [-]

M: re-use factor Taq enzyme during annealing phase [-]
N: complexity [-]
N_{base}: number of base pairs to be elongated [-]
N_r: molar flux species in r-direction [mol/m^2/s]
n: cycle number [-]
$n_{avogadro}$: Avogadro's number [6.022*10^{23} /mol]
n_{cycle}: number of templates captured on spot surface [-]
n_{probes}: number of probes in spot [-]
R_{max}: elongation rate constant [mol/m^3/s]
$R_{max,55°C}$: elongation rate constant at 55 °C [mol/m^3/s]
$R_{max,72°C}$: elongation rate constant at 72 °C [mol/m^3/s]
r: radial co-ordinate measuring the distance from the centre of the spot surface [m]
r_{reach}: reach of diffusion process measured from dome surface [m]
t: time [s]
t_{hyb}: annealing/hybridization time [s]
$t_{elongation}$: elongation time [s]
θ: fraction of hybridized probes [-], spherical co-ordinate [rad]
φ: spherical co-ordinate [rad]
τ: time constant annealing process [s]

2 Mathematical modelling and main assumptions

We split the mathematical modelling of the Real Time Array PCR process in a number of steps:

- First we list the chemical reactions taking place during the different temperature steps in order to define the different reactions approximately right, without going into too much detail. Here we refer to (**Wetmur and Davidson, 1968; Schnell et al., 2000; Whitney et al., 2004; Gevertz et al., 2005; Booth et al., 2010**).
- Then we give the different rate equations describing the time evolution of the chemical reaction equations listed.
- We solve the equations describing the rate of change of the different species in the bulk.
- The bulk concentrations will be used to solve the kinetic equation describing the hybridization process. Here we will make the assumption that only free single stranded DNA will hybridize to capture probes immobilized at the array surface. Although the hybridization site and the primer site of the amplicon do not overlap, due to steric hindrance it is most unlikely that the secondary and/or tertiary complexes will react with the capture probes.

Typically, the RTA PCR process starts with a hot start which has two functions: next to the activation of the hot-start enzyme, it ensures that all dsDNA especially the template molecules are denatured. This situation will be the initial condition for the first cycle of annealing in the bulk and hybridization at the microarray surface during 120 seconds at 55°C, elongation during

40 seconds at 72 °C, followed by a short denaturation step during 20 seconds at 95 °C (see also figure 1). The now changed concentrations of the different species will be the initial conditions for the next round of annealing and hybridization, elongation and denaturation and so on. The main result of our analysis will be the evolution of the number of hybridized targets on a spot of the microarray at the end of the annealing step, determined cycle after cycle. We also will follow in course of time the number of amplicons captured during the whole annealing/hybridization step.
It should be noted that initially the concentration of templates is very low. A template is typically a long DNA fragment of which during amplification only a small part, called the amplicon, will be amplified. After a number of cycles the concentration of original templates is negligible with respect to the concentration of short stranded amplicons.

The main assumptions of our analysis are:

- Only free single stranded DNA hybridizes with complementary capture probes immobilized on the microarray surface
- We consider only forward reactions
- Primer–dimer formation is neglected
- The formation of tertiary complexes of binary complexes with enzymes is much faster than the anneal reactions, tertiary complexes are elongated also fast delivering dsDNA and enzymes that can react, shifted in time, with other binary complexes many times.
- The Taq enzyme driven consumption of dNTP's during elongation is governed by Michaelis-Menten kinetics
- Surface hybridization follows Langmuir kinetics

We have included

- Different annealing rate constants for the formation of binary complexes and renaturation during the annealing phase
- Elongation takes place during the annealing phase and the elongation phase.
- Reuse of enzymes during annealing phase.

3.1 Basic reaction equations

During denaturation dsDNA splits into equal amounts of single stranded ssDNA (sense and antisense). In the following sense ssDNA is referred to as species A and likewise antisense ssDNA as species B (the red dots indicate the presence of a fluorophore attached to species A):

$$dsDNA \rightarrow A + B \tag{1}$$

After denaturation, the temperature is lowered to the annealing temperature (e.g. 55°C) and a number of processes start in parallel. In the bulk ssDNA reacts with primers to form binary complexes, moreover species A and species B react with each other again (renaturation) to form dsDNA (**Whitney et al., 2004**). All reverse primers are labelled. We have assumed that the primers are designed such that they do not form primer dimers. So we have:

$$\begin{aligned} A + B &\rightarrow dsDNA \\ A + primer_{forward} &\rightarrow complex_1 \\ B + primer_{reverse} &\rightarrow complex_2 \end{aligned} \tag{2}$$

During initial cycling, the complex formation is the preferred reaction because of the vast excess of primers compared to the initial load of templates. At the end of the Real Time PCR process the situation is reverse, the preferred reaction the formation of dsDNA because the system is running short of primers. More extended descriptions of the reactions involved in Real Time PCR can be found in (**Gevertz et al., 2005; Booth et al., 2010**).

The binary complexes react with polymerase enzymes to form tertiary complexes:

$$complex_i + polymerase \rightarrow tertiary\ complex_i\ ,\ i = 1{,}2 \tag{3}$$

Already during the annealing phase elongation of primers starts at a low rate (40% of maximal rate, see product information of (**Invitrogen, 2011**)):

$$tertiary\ complex_i + dNTP \longrightarrow dsDNA + polymerase\ ,\quad i = 1{,}2 \tag{4}$$

The polymerase liberated by this reaction will be involved again, shifted in time, in other reactions described by (3) and (4).

On the spot surface we envision the capturing of only free species A:

$$A + capture\ probe_{surface} \rightarrow complex_{surface\ without\ primer} \quad (5)$$

All other reactions involving capture probes with binary or tertiary complexes are unlikely because of the steric hindrance effect of the primers and enzymes on the hybridization reaction, especially for the short strands considered in this paper (molecular weight binary complex (100 bases amplicon and 30 bases primer) roughly 60-70 kDa, Taq enzyme 94 kDa). At the elongation temperature binary complexes and complexes formed at the array surface will most probably melt. The tertiary complexes still left in the solution are sufficiently stable and will be elongated, delivering the final yield of the PCR process.
Next the system will be heated to 95 °C, all double stranded DNA molecules in the bulk denaturize. Also complexes in the bulk that still did not elongate fully will be split into ssDNA and longer primers (**Whitney et al., 2004**). In our analysis we assume full elongation and neglect the possible presence of incompletely elongated primers. The temperature is lowered to 55°C and the whole procedure is repeated again and again, which we limit here to 60 cycles. After each anneal/hybridization step the captured molecules on the surface of the microarray are "counted" by measuring the fluorescence per spot.

Two other reactions must be mentioned:

- During temperature cycling part of the polymerase will lose its activity (**Sambrook and Russell, 2001, Invitrogen product data, 2011**). The enzyme half time at 95 °C is 40 minutes and at 97.5 °C only 5 minutes. During thermal cycling the mix stays at 95 °C for 20 seconds per cycle, including the hot start and 60 cycles in total 30 minutes. We estimate per cycle an activity decrease by about 1 %. This is expected to be higher compared to qPCR due to the fact that the temperature control of the RTA PCR set-up may not accurate enough to guarantee that the temperature always is at most 95 °C. Also part of the enzymes may be caught by the walls of the reaction chamber and will lose activity (**Erill et al., 2003; Potrich et al., 2010**). Different numbers of the degradation of the enzyme are listed in literature (**Gevertz et al., 2005; Whitney et al., 2004**). In this paper we will use a total loss of enzyme activity of 2% per cycle in our analysis following (**Whitney et al., 2004**).
- During thermocycling the capture probes may be damaged or detached, leading to a lower number of capturing sites on the microarray surface. Another mechanism can be envisioned as well: fouling of the microarray surface. We assume that no degradation of capture probes is the standard situation. We will give an example what happens when an increasing percentage of the capture probes lose their capturing ability per cycle.

3.2 Rate equations

3.2.1 Bulk reactions

We start with analysing the bulk reactions taking place in the PCR chamber first, so for the time being we neglect the influence of the hybridization reaction between targets and capture probes at the microarray surface. The concentrations of species A and B decrease in course of time according to (**Wetmur and Davidson, 1968, Whitney et al., 2004**):

$$\frac{\partial c_A}{\partial t} = -kc_A c_{pF} - k_{dsDNA} c_A c_B, \quad \frac{\partial c_B}{\partial t} = -kc_B c_{pR} - k_{dsDNA} c_A c_B \tag{6}$$

The consumption of species A is governed by two processes, the formation of complexes of amplicons with primers (controlled by the rate constant k) and the formation of dsDNA (controlled by the rate constant k_{dsDNA}). All the time it holds (primer-dimer formation neglected, PCR reaction is symmetric in species A and B):

$$c_A + c_{pF} = c_{p0} + c_{template} \approx c_{p0}, \qquad c_B + c_{pR} = c_{p0} + c_{template} \approx c_{p0}, \qquad c_A = c_B \tag{7}$$

Note that c_{p0} is the concentration of the primers at the start of the process. The initial concentration of the templates in the PCR mix $c_{template}$ is very small. In course of the process the initial concentration of templates can be neglected. These conditions cause the second order reaction equations to turn into Riccati type of equations (**Szabo 1959**):

$$\frac{\partial c_A}{\partial t} = -kc_{p0} c_A + (k - k_{dsDNA}) c_A^2, \quad \frac{\partial c_B}{\partial t} = -kc_{p0} c_B + (k - k_{dsDNA}) c_B^2 \tag{8}$$

The concentration denatured dsDNA follws from:

$$\frac{\partial c_{dsDNA}}{\partial t} = k_{dsDNA} c_A c_B \tag{9}$$

Because of conservation of species (either A or B) the concentrations of secondary complexes read (c_0 concentration of either species A or B at the beginning of the annealing/hybridization phase):

$$c_{complex_1}(t) = c_0 - c_A(t) - c_{dsDNA}(t)$$
$$c_{complex_2}(t) = c_0 - c_B(t) - c_{dsDNA}(t) \quad (10)$$

Following (**Whitney et al., 2004)**, the formation of tertiary complexes is fast, especially during the start of the PCR process because of the excess of enzymes with respect to the number of amplicons. These tertiary complexes react further to form dsDNA and enzymes. During elongation, the rate of consumption of dNTP's used for elongation is described by the so-called Michaelis-Menten kinetics (**Schnell et al., 2000; Gevertz et al., 2005; Truskey et al., 2010**):

$$\frac{dc_{dNTP}}{dt} = -\frac{R_{max}\, c_{dNTP}}{K_m + c_{dNTP}} \quad (11)$$

Where R_{max} is the maximum reaction rate and K_m the Michaelis constant for the enzyme controlled process of adding dNTP's to the tertiary complexes.
In case the enzymes lose activity during cycling, $R_{max}(n)$ is given by (n cycle number and f_{TAQ} fraction decrease activity):

$$R_{max}(n) = (1 - f_{TAQ})^n R_{max} \quad (12)$$

In our analysis we will use two values for R_{max}, namely one valid for 72 °C: $R_{max,72\,℃}$ and another one for following the elongation of the primers at the anneal temperature of 55 °C: $R_{max,55\,℃}$.

3.2.2 Surface reactions

In the neighbourhood of the spots of the microarray the diffusion is essentially three dimensional. We can simplify this picture by assuming the concentration profile to be axisymmetric. As a thought experiment we replace the flat spot by a spherical cap (dome) with the same surface area (keeping the surface density of capture probes identical); the only co-ordinate that remains is the distance r from the centre of the spherical cap (spherical symmetry, see figure 2). The geometrical data of the dot radius b and the radius of the spherical dome a are related by:

$$2\pi a^2 = \pi b^2 \rightarrow a = \frac{b}{\sqrt{2}} = \frac{1}{2} b\sqrt{2} \quad (13)$$

The components of the diffusion equation (being Fick's second law) are defined with respect to a spherical co-ordinate system: r, θ, φ (**Bird et al., 2002**) . The only component that remains after carrying out the steps outlined above is the r-component.

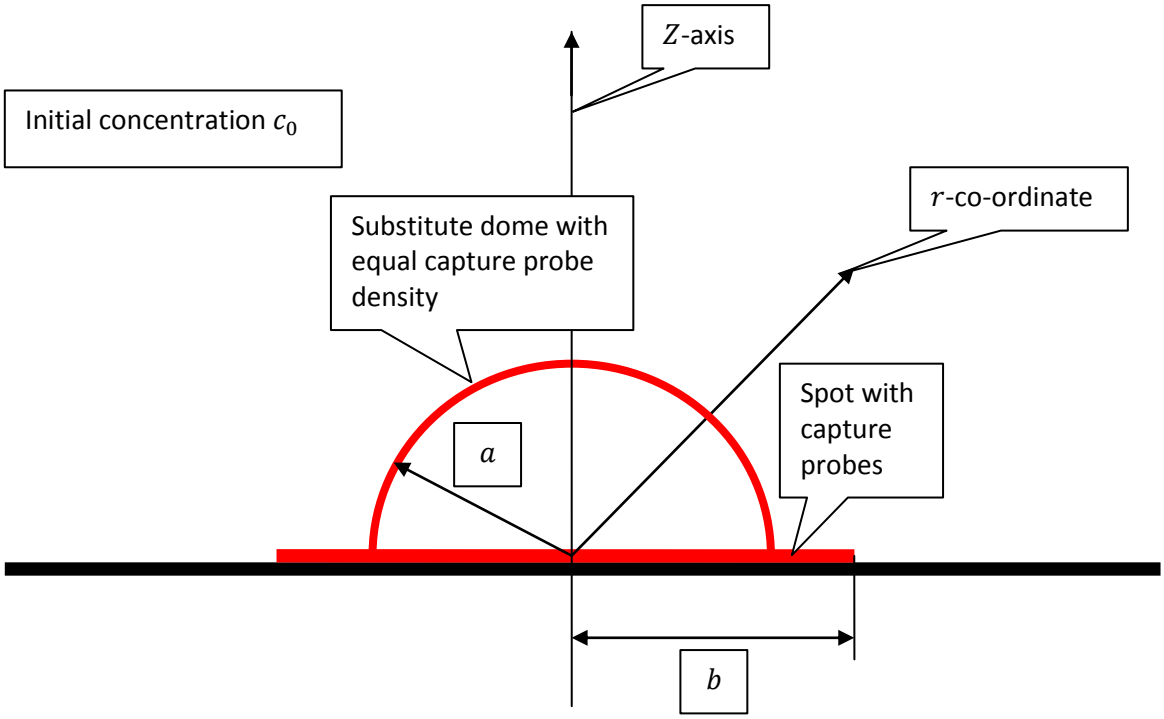

Figure 2 Definition of substitute semi-spherical dome carrying the capture probes. The surface areas of the spherical cap and the original spot surface are equal.

In order to understand the hybridization kinetics at the spot surface we use the Langmuir kinetic model (**Gao et al., 2006**; **Fiche et al., 2007, Mocanu et al., 2008; Squires et al., 2008; Mocanu et al., 2009**) (θ fraction of hybridized probes at the spot surface with respect to the total number of capture probes, k_{ass} and k_{diss} association and dissociation rate constants and $c_{r=a}$ the concentration of targets in the bulk at the surface of the spot):

$$\frac{d\theta}{dt} = k_{ass} c_{r=a}(1-\theta) - k_{diss}\theta \tag{14}$$

Initially (in terms of number of cycles) the fraction of hybridized targets is very small (no competition) and the Langmuir kinetic equation can be approximated by:

$$\frac{d\theta}{dt} = k_{ass} c_{r=a} \tag{15}$$

Which equation can be rewritten in terms of molar flux as:

$$\frac{d\theta n_{probes}/n_{avogadro}}{2\pi a^2 dt} = -N_{r=a} = k_{ass} c_{r=a} \frac{n_{probes}}{n_{avogadro}} \frac{1}{2\pi a^2} \tag{16}$$

In the bulk the molar flux of the targets is given by (Fick's first law (**Bird et al., 2002**)):

$$N_r = -\mathcal{D} \frac{\partial c}{\partial r} \tag{17}$$

The flux boundary condition at $r = a$ is given by:

$$\frac{\partial c}{\partial r}|_{r=a} = \frac{k_{ass}}{\mathcal{D}} \frac{n_{probes}}{n_{avogadro}} \frac{1}{2\pi a^2} c_{r=a} = h c_{r=a} \tag{18}$$

$$h = \frac{k_{ass}}{\mathcal{D}} \frac{n_{probes}}{n_{avogadro}} \frac{1}{2\pi a^2}$$

In case a certain percentage of the probes become inactive during thermal cycling, this will affect the radiation condition since its value depends on the number of probes (with f_{probes} the fraction degradation, here it is tacitly assumed that k_{ass} does not depend on the surface concentration):

$$\frac{\partial c}{\partial r} = h(1 - f_{probes})^n c_{r=a} \tag{19}$$

The concentration of targets is the concentration of free ssDNA.

3.3 Solutions of the rate equations

In this paragraph, the solutions for the Real Time PCR process (section 3.3.1) and for the Real Time Array PCR process (section 3.3.2) are derived. Section 3.3.3 describes additional material data needed for solving the equations. Typical examples of the outcomes and the results of a parameter study are given in the results paragraph 4.

3.3.1 Solutions for Real Time PCR

The rate at which the concentrations of both species A and B decrease are given by Riccati type of equations (8) of which the solutions are (**Szabo, 1959**):

$$c_A = \frac{c_{A0}}{\left[1 - \frac{c_{A0}(k - k_{dsDNA})}{kc_{pO}}\right] e^{kc_{po}t} + \frac{c_{A0}(k - k_{dsDNA})}{kc_{pO}}} \quad ,$$
$$c_B = \frac{c_{B0}}{\left[1 - \frac{c_{B0}(k - k_{dsDNA})}{kc_{pO}}\right] e^{kc_{po}t} + \frac{c_{B0}(k - k_{dsDNA})}{kc_{pO}}} \tag{20}$$

(c_{A0} and c_{B0} are the concentrations of species A and B at the beginning of the annealing/hybridization phase).
Because of the fact that the PCR reaction is symmetric in species A and species B at the start of each hybridization/annealing step it holds:

$$c_{A0} = c_{B0} = c_0 \tag{21}$$

Upon substitution of the exact solution (20) into the rate equation for dsDNA (9) we find for the concentration of dsDNA as function of time:

$$c_{dsDNA} = \frac{c_0^2}{c_{p0}} \frac{k_{dsDNA}}{k} \left(\frac{kc_{p0}t}{c^{*2}} - \frac{\ln\left((1 - c^*)e^{kc_{p0}t} + c^*\right)}{c^{*2}} + \frac{1}{c^*}\left(\frac{1}{(1 - c^*)e^{kc_{p0}t} + c^*} - 1\right) \right) \tag{22}$$
$$c^* = \frac{c_0(k - k_{dsDNA})}{kc_{pO}}$$

For long times the concentration of dsDNA goes to a constant value given by:

$$t \to \infty\colon\ c_{dsDNA} \to \frac{1}{2}\frac{c_0^2}{c_{p0}}\frac{k_{dsDNA}}{k} \tag{23}$$

The concentrations of $complex_1$ and $complex_2$ can be calculated using equations (10).

As mentioned earlier the enzymes react fast with the binary complexes, to form tertiary complexes. These tertiary complexes react fast with the dNTP's available is excess in the solution to form dsDNA. After full elongation the enzyme is freed and is available again for forming tertiary complexes with available binary complexes.
At the end of the annealing/hybridization phase at $t = t_{hyb}$, the temperature is raised to the elongation temperature, all anneal reactions stop, captured amplicons will detach from the array surface and binary complexes (when still present) will melt.

The rate of consumption of dNTP's is given by the Michaelis-Menten equation (11).

After the elongation phase the temperature is raised again to 95 °C and all dsDNA molecules are denatured.

The amplification process is subjected to four limiting effects, namely:

- the anneal time and elongation time are too short to elongate all available tertiary complexes,
- the depletion of primers available for making complexes,
- the depletion of enzymes available for forming tertiary complexes,
- the depletion of dNTP's that have been consumed during elongation.

For all cases discussed in this paper we assume that the PCR process stops because of depletion of primers and/or enzymes and that dNTP's are present in more than sufficient excess.
Elongation takes place already during the annealing phase and at a higher rate during the elongation phase.
The concentration of tertiary complexes at the end of the annealing phase becomes:

$$c_{tertiary_i}(t_{hyb}) = c_{complex_i}(t_{hyb}) - \frac{R_{max,55\,^\circ\mathrm{C}}(n)t_{hyb}}{2N_{base}}\,\frac{c_{dNTP}}{K_m + c_{dNTP}} \tag{24}$$

(c_{dNTP} denotes the concentration of each of the four dNTP's during process. Because of the excess concentration the concentration of dNTP's is a slowly decreasing function of time, the mean value at the start of the annealing process is used here, assuming equal numbers of dATP,

dCTP, dGTP and dTTP in amplicons and primers. $R_{max,55\,℃}(n)$ is defined by formula (12)). When the concentration calculated according to (24) is negative full elongation has been reached already during the annealing/hybridization phase. If not, elongation continues during the elongation phase. At the end of the elongation phase the concentration tertiary complexes follows from:

$$c_{tertiary_i}(t_{elongation}) = c_{complex_i}(t_{hyb}) - \frac{R_{max,55\,℃}(n)t_{hyb}}{2N_{base}} \frac{c_{dNTP}}{K_m + c_{dNTP}} - \frac{R_{max,72\,℃}(n)t_{elongation}}{2N_{base}} \frac{c_{dNTP}}{K_m + c_{dNTP}} \tag{25}$$

Likewise as for the annealing we can conclude that when the concentration tertiary complexes at the end of the elongation phase is negative, full elongation of the primers has been achieved ($E_{elongation} = 1$). If not, there is no complete elongation and the elongation factor $E_{elongation}$ is defined by:

$$E_{elongation} = \frac{c_{complex_i}(t_{hyb}) - c_{tertiary_i}(t_{elongation})}{c_{complex_i}(t_{hyb})} \tag{26}$$

With this in mind the effect of the elongation process of the bulk PCR in terms of the concentration of species A at the end of the denaturation phase at 95 °C can be described by:

$$c_A = c_A(t_{hyb}) + c_{dsDNA}(t_{hyb}) + E_{elongation}\{c_{complex_1}(t_{hyb}) + c_{complex_2}(t_{hyb})\} + (1 - E_{elongation})c_{complex_1}(t_{hyb}) \tag{27}$$

Because of symmetry a similar expression holds true for species B.
Let us discuss the effect of the depletion of primers. The above description holds true as long as:

$$c_{complex_i} < c_{p0} - c_0, \;\; i = 1,2 \tag{28}$$

When not enough primers are available to anneal to all strands available we get after elongation:

$$c_A = \; c_B = 2c_0 - c_{p0} + 2E_{elongation}(c_{p0} - c_0) + (1 - E_{elongation})(c_{p0} - c_0) \tag{29}$$

Another limiting condition is the amount of available enzyme molecules. Here the fact that enzymes can be reused many times must be taken into account. This will be modelled by introducing a reuse factor M. The rate at which an enzyme is able to build dNTP's into a tertiary complex is 20-100 dNTP/s at 72 °C (for 55 °C the rate is about 0.4 of the value given at 72 °C (**Invitrogen, 2011**)). That means that the elongation of a primer just takes a few seconds. The effect of M is crucial for understanding the elongation process during annealing, because during that phase one enzyme can be used many times. At the higher temperature of 72 °C most probably the binary complexes have been melted, so the enzymes can only elongate the tertiary complexes once. The value of M will be discussed in chapter 3.3.3.
The effect of the depletion of enzymes follows a similar scheme as discussed for the depletion of the primers. The above description holds true as long as:

$$c_{complex_i} < M c_{TAQ}/2, \;\; i = 1,2 \tag{30}$$

When not enough enzymes are available to form tertiary complexes with all binary complexes available we get after elongation:

$$c_A = \; c_B = c_0 - M\frac{c_{TAQ}}{2} + 2E_{elongation}M\frac{c_{TAQ}}{2} + (1 - E_{elongation})M\frac{c_{TAQ}}{2} \tag{31}$$

The efficiency of a PCR step is defined by (n cycle number):

$$E(n) = \frac{c_A}{c_0} - 1 \tag{32}$$

3.3.2 Solutions for Real Time Array PCR

Now we consider the hybridization of amplicons, in our case single stranded species A, to capture probes immobilized on the array surface. Free species A is consumed by the renaturation of species A and species B to dsDNA and by the formation of complexes.
We model the decrease in bulk concentration of species A by means of a second order reaction and the diffusion equation becomes (Fick's second law (**Bird et al., 2002**) combined with equation (8)):

$$\frac{\partial c_A}{\partial t} = \mathcal{D}\frac{1}{r^2}\frac{\partial}{\partial r}r^2\frac{\partial c_A}{\partial r} - k c_{p0} c_A + (k - k_{dsDNA})c_A^2 \tag{33}$$

The rate constants k and k_{dsDNA} are of equal magnitude and during most of the thermal cycles $c_A \ll c_{p0}$, so the last term of the right hand side of equation (33) can be neglected:

$$\frac{\partial c_A}{\partial t} = \mathcal{D}\frac{1}{r^2}\frac{\partial}{\partial r}r^2\frac{\partial c_A}{\partial r} - kc_A c_{p0} \tag{34}$$

We can solve for the reaction part:

$$c_A = c_{A0}e^{-kc_{p0}t} \tag{35}$$

We put as solution for the diffusion equation including the bulk chemical reaction:

$$c_A = f(r,t)c_{A0}e^{-kc_{p0}t} \tag{36}$$

Where $f(r,t)$ follows from:

$$\frac{\partial f(r,t)}{\partial t} = \mathcal{D}\frac{1}{r^2}\frac{\partial}{\partial r}r^2\frac{\partial f(r,t)}{\partial r} \tag{37}$$

With initial condition $t = 0, r > a, f(r,t) = 1$, and the flux condition for $r = a$:

$$\frac{\partial f(a,t)}{\partial z} = \frac{k_{ass}}{\mathcal{D}}\frac{n_{probes}}{n_{avogadro}}\frac{1}{2\pi a^2}f(a,t) = hf(a,t) \tag{38}$$

The solution of the differential equation (37) subjected to initial and boundary conditions (38) can be found in (**Carslaw and Jaeger, 1959**). The concentration as a function of time now becomes (h' being a short hand writing defined below):

$$\frac{c_A}{c_{A0}} = e^{-kc_{p0}t}\left[1 - \frac{ha^2}{r(ah+1)}\left\{\operatorname{erfc}\frac{r-a}{\sqrt{4Dt}} - e^{h'(r-a)+h'^2Dt}\operatorname{erfc}[\frac{r-a}{\sqrt{4Dt}} + h'\sqrt{Dt}]\right\}\right] \tag{39}$$

$$h' = h + \frac{1}{a}$$

And the concentration just above the surface of the dot:

$$\frac{c_{A,r=a}}{c_{A0}} = e^{-kc_p t}\left[1 - \frac{h}{h'}\left\{1 - e^{h'^2 Dt}\,\mathrm{erfc}(h'\sqrt{Dt})\right\}\right] \tag{40}$$

The total number of captured targets can be found by integration by parts of (15):

$$\begin{aligned} n_{cycle} &= \theta n_{probes} = \int_0^{t_{hyb}} \frac{d\theta n_{probes}}{dt}\,dt \\ &= k_{ass} c_{A0} n_{probes} \int_0^{t_{hyb}} e^{-kc_{p0}t}\left[1 - \frac{h}{h'} + \frac{h}{h'} e^{h'^2 Dt}\,\mathrm{erfc}(h'\sqrt{Dt})\right]\,dt \end{aligned} \tag{41}$$

The final result reads (with $\xi_{hyb} = h'\sqrt{Dt_{hyb}}$):

$$\begin{aligned} n_{cycle} = {} & k_{ass} c_{A0} n_{probes}\left[\frac{1}{kc_{p0}}\left(1 - \frac{h}{h'}\right)\left(1 - e^{-kc_{p0}t_{hyb}}\right)\right. \\ & \left. + \frac{h}{h'}\frac{1}{(-kc_{p0} + h'^2 D)}\left\{e^{\frac{(-kc_{p0} + h'^2 D)}{h'^2 D}\xi_{hyb}^2}\,\mathrm{erfc}\,\xi_{hyb} - 1\frac{1}{\sqrt{\frac{kc_p}{h'^2 D}}}\,\mathrm{erf}(\xi_{hyb}\sqrt{\frac{kc_{p0}}{h'^2 D}})\right\}\right] \end{aligned} \tag{42}$$

3.3.3 Material data

The annealing (forming complexes of dsDNA with primers and renaturation of ssDNA to dsDNA) is described by second order reactions.
For k the Wetmur/Davidson relation (**Wetmur and Davidson, 1968**) will be used:

$$k = 300\frac{\sqrt{L}}{N}\ [\frac{\mathrm{m}^3}{\mathrm{mol\ s}}] \tag{43}$$

This relation holds true under strict conditions (salt concentration 1 M [Na^+] and 25 °C below the melting temperature). The value of k strongly depends on the salt concentration. The number of bases is denoted by L. The value of N is referred to as the complexity, the number of base pairs in non-repeating sequences, for short strands: $N = L$. The number of nucleotides in the amplicons in our analysis is about 100. In case strands of different lengths anneal, the data for the shortest should be entered (**Anderson, 1999**), which is the length of the primers (20-40 bases) leading to the conclusion that the rate constant for annealing is about 50-70 m^3/mol/s (somewhat higher values but of the same order of magnitude for comparable cases are reported by (**Wang and Drlica, 2003**)). In our calculation we will use $k = 60$ m^3/mol/s and for the renaturation reaction with strands of 100 bases, $k_{dsDNA} = 30$ m^3/mol/s. It should be mentioned that these values are supported by experimental evidence, because usually the PCR efficiency is close to 100 %, leading to the conclusion that within 120 seconds annealing is not a limiting factor. Higher values of k lead to PCR efficiencies even closer to 100 %.
In (**Gao et al., 2006**) data are reported that suggest that the surface hybridization reaction is 20-30 times slower than the bulk reaction, we use here:

$$k_{ass} = k/20 \tag{44}$$

This factor reflects first of all that because of the presence of the wall of the PCR chamber diffusion towards the capture probes is limited to a half space. Moreover the capture probes are immobilised to the array surface, and because of steric hindrance the association reaction between amplicons and capture probes will be strongly hampered.

One unit is defined as the amount of enzymes which will convert 10 nmoles of dNTP's to an acid-insoluble form in 30 min at 72°C under the assay conditions. From this definition we can derive the rate constant for the elongation process (addition of dNTP's), driven by 1 EU polymerase:

$$R_{max,72\,℃} = \frac{10 * 10^{-9}}{30 * 60}\frac{1}{V_{PCR\ chamber}} = 2.22 * 10^{-4}\ [\mathrm{mol/m^3/s}] \tag{45}$$

The value at 55 °C is 40% of the value given above ($R_{max,55\,°C} = 8.89 * 10^{-5}\ [\mathrm{mol/m^3/s}]$.

A key number in our calculations is the number of Taq enzyme molecules per unit. We refer to (**Sprangler et al., 2009**) and have used 8*10^{10} enzymes per unit. Using the definition of a unit we can calculate the number of dNTP's added per unit time, for the number of enzymes per unit given here, this number appears to be 42 dNTP/s at 72 °C and 17 dNTP/s at 55 °C. This means that for 70 bases to be added it takes 1.67 seconds at the elongation temperature and 4.2 seconds at 55 °C (anneal temperature). This leads to the conclusion that for 55 °C (anneal temperature): $M = 28.8$.
So the apparent number of enzyme molecules that is involved in the elongation process during annealing is the number of enzyme molecules per unit times M: 2.3*10^{12}. During the elongation phase the temperature is so high that most probably all binary complexes have been melted. Tertiary complexes that did not react during annealing will be elongated. The Taq enzymes that are freed will not find binary complexes anymore and will be used once.

The value of K_m, per each dNTP a value of 10-15 *10^{-3} mol/m^3 is found in literature (**Landgraf and Wolfs, 1993**). We have entered 15*10^{-3} mol/m^3.

The diffusion coefficient of single stranded DNA with 100 bases at 55 °C is taken equal to (**Reinick et al., 2010**):

$$\mathcal{D} = 8.54 * 10^{-11}\ [\frac{\mathrm{m}^2}{\mathrm{s}}] \tag{46}$$

4 Results and discussion

The model developed in this paper allows for a parameter study to investigate the influence of the different parameters involved around a standard protocol.
We define as standard protocol an initial load of 250,000 templates, $0.3*10^{-3}$ mol/m^3 primer concentration (both reverse and forward primer), 0.2 mol/m^3 dNTP's (for each of the four dNTP's), 1 EU enzyme load, a decay rate of Taq enzyme activity of 2% per cycle and a zero decay rate per cycle for the capture probe activity. Timing is 120 seconds annealing/hybridization, 40 seconds elongation and 20 seconds denaturation. Total number of cycles equals 60. Material data are listed in paragraph 3.3.3.

Figure 3 shows how the concentrations of different species, such as species A, forward primer, Taq enzyme (concentration given as $Mc_{Taq}/2$) develop during thermal cycling.

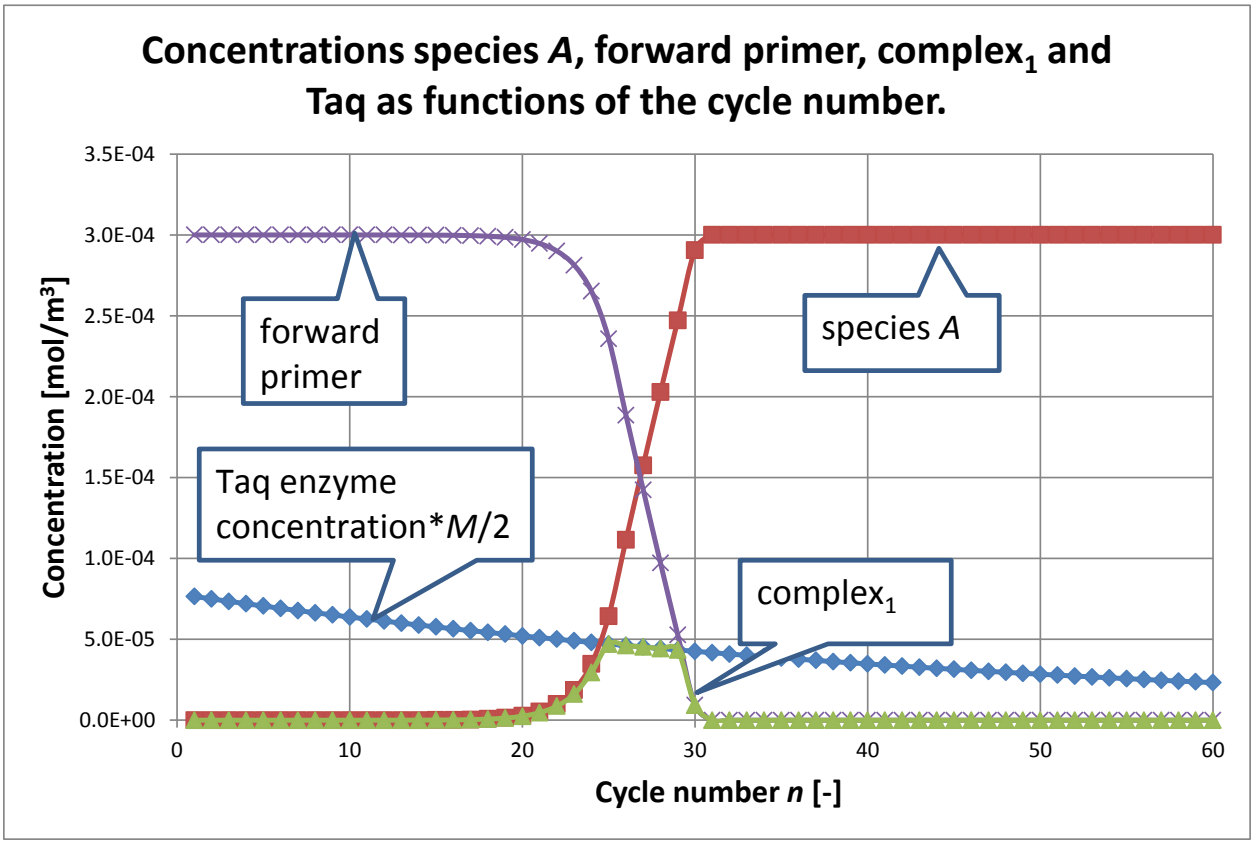

Figure 3 Evolution of concentration of species A, forward primer, $complex_1$ and Taq enzyme during thermal cycling for the standard protocol (note that we have given here half the concentration of Taq times the reuse factor M, equation (30)).

The values of the elongation factor and the PCR efficiency both as functions of the cycle number are shown in figure 4.

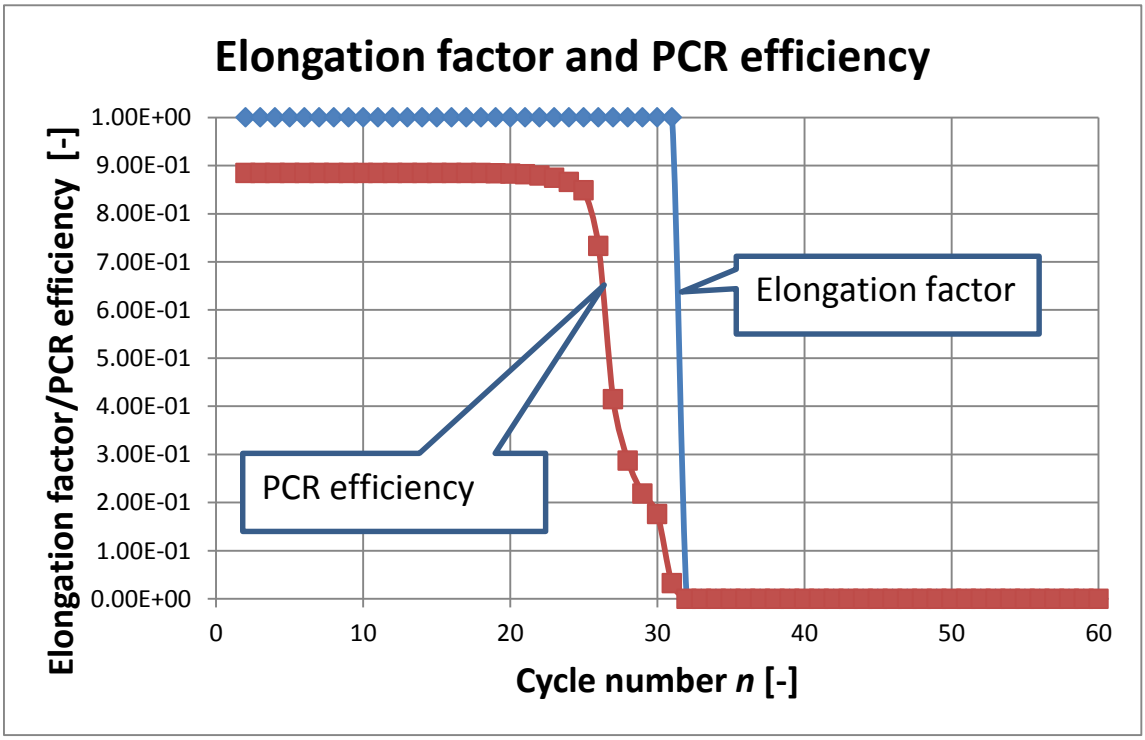

Figure 4 Elongation factor (defined by formula (26)) and PCR efficiency (defined by formula (32)) for the standard case as functions of the cycle number. The elongation factor gives the extent to which all available primers in tertiary complexes have been elongated (1 all primers elongated, 0 no elongation). The PCR efficiency includes all the effects, such as incomplete annealing and renaturation.

From figure 3 and 4 we learn several features of the PCR process as modelled in chapter 3. First of all looking to the concentration of species A as a function of the cycle number , the general behaviour as measured in qRT PCR is observed. For the template load of 250,000 the C_t value is around 20. At a certain moment in time either primers or Taq enzymes are running short for all available strands to form binary and tertiary complexes during annealing. That is clearly visible in figure 3: the complex concentration increases up to cycle number 25, from cycle number 26 the complex concentration decreases and follows the apparent Taq concentration curve ($Mc_{Taq}/2$) and from cycle number 29 the complex concentration decreases steeply and coincides with the primer concentration curve. Up to the point where the availability of either primers or Taq enzymes becomes the limiting factor for full amplification, the theory developed in chapter 3 is valid as far as the concentration of species A and dsDNA as functions of time are concerned. From equation (42) which is the result of the analysis of the hybridisation kinetics,

we can conclude that the total amount of amplicons captured scales with the concentration of free species A at the beginning of the annealing phase. This means that the hybridisation curve as a function of the cycle number has the same shape as the amplification curve, provided that the capture probes do not wear.
With reference to figure 4 and formula (26) the elongation factor curve indicates whether the enzymes present are able to elongate all the available primers in the tertiary complexes. From cycle number 31 on there are no primers anymore and the elongation process stops. The PCR efficiency includes the effect of the elongation factor but also the effects that annealing has not been complete and that for higher cycle numbers more and more dsDNA is formed instead of complexes.

In figure 5 the concentration profiles above the dot (modelled as a spherical dome) are given.

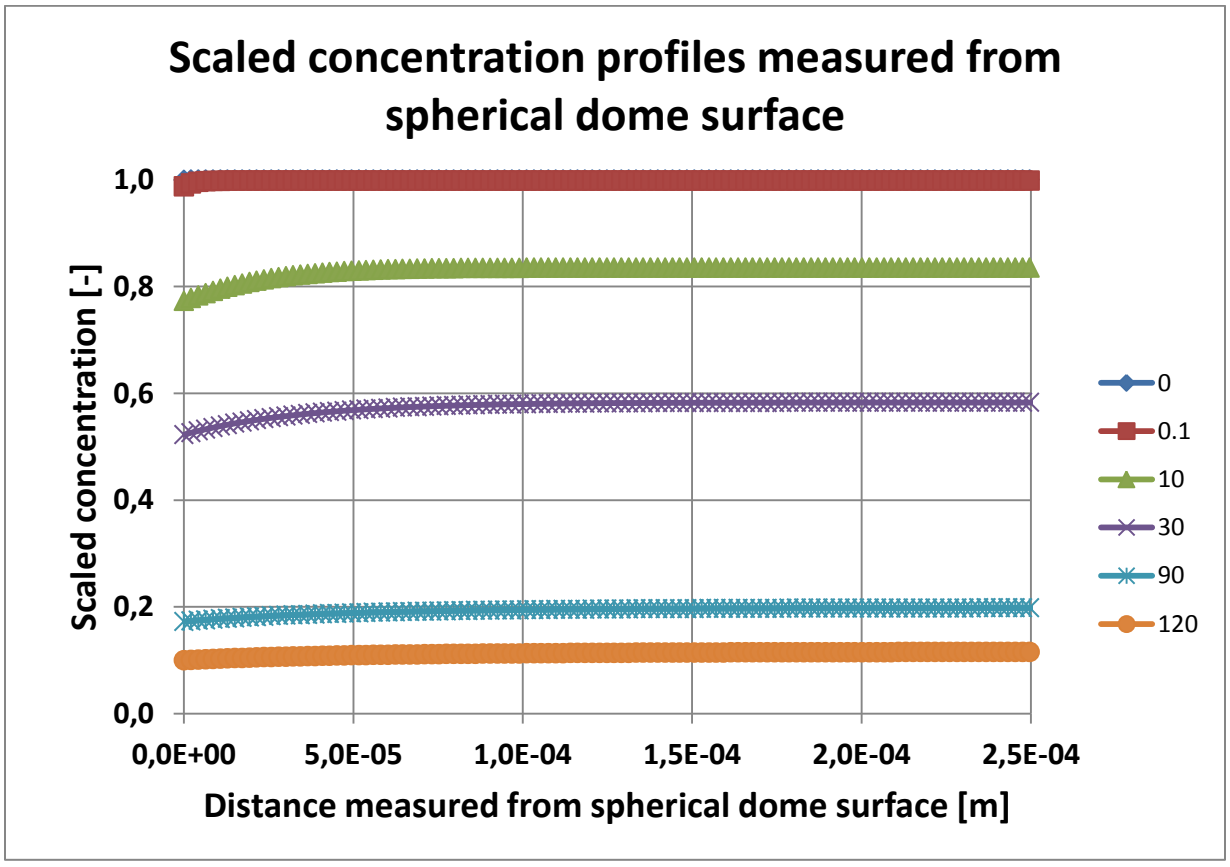

Figure 5 Concentration profiles above the dot, modelled as a spherical dome. The distances are measured from the dome surface. The times at which the concentration profiles are calculated are given in the legend (in seconds).

In course of the annealing time the concentration of free species A in the bulk decreases, reducing the concentration gradient close to the dot surface, reducing the rate at which

amplicons bind to capture probes. At the end of the annealing phase the concentration of free species A has been reduced to 10%.
The penetration depth or reach of the diffusion can be estimated by using the following approximate formula (**Carslaw and Jaeger, 1959; Bird et al., 2002**):

$$r_{reach} = \sqrt{\mathcal{D}t_{hyb}} \tag{47}$$

Upon substituting the data of the standard process the reach equals 100 µm measured from the surface of the dome, which value complies well with the findings displayed in figure 5.
We can use this number to estimate the asymmetry in concentrations between species A and B. Species A can bind to the surface of the microarray, while species B cannot. With equation (42) we can calculate the number of amplicons per cycle that hybridize with capture probes on the array surface. With the reach above defined we can calculate the ratio of the concentration of hybridized amplicon within reach and the concentration of species A at the start of the anneal process by (note that n_{cycle} scales with c_{A0}):

$$\frac{c_{hybridized\ amplicons}}{c_{A0}} = \frac{n_{cycle}}{n_{avogadro}} \frac{1}{c_{A0}\frac{2}{3}\pi\{(r_{reach}+a)^3 - a^3\}} \tag{48}$$

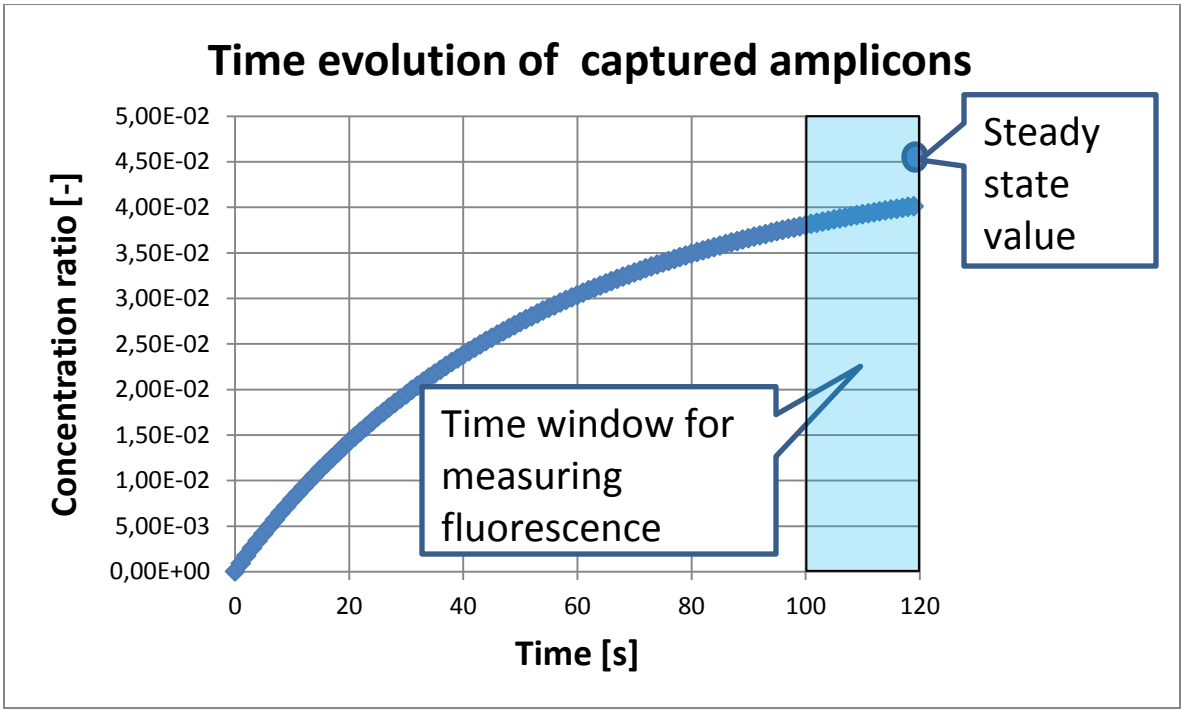

Figure 6 Ratio of number of amplicons reacted with surface probes given as concentration within reach and the concentration of species A at the start of the annealing process (48) as function of time. The steady state value is 0.0452 (1000 seconds). The shaded area is the time window used for fluorescence detection.

For our case this ratio appears to be 4.5 % (independent on cycle number as all scales with the concentration c_{A0}), which implies that asymmetry is small and can indeed be neglected.

The timing of the surface hybridization reaction is shown in figure 6. The timing of the hybridization reaction follows the timing of the annealing. Considering equation (36) we can define a time constant τ given by:

$$\tau = 1/(kc_{p0}) \tag{50}$$

In our case $\tau = 56\ s$, which means that after 56 seconds about 63 % of the reaction has taken place, at double time 86 % and for 120 seconds about 90%. As shown in figure 6 the hybridization reaction has not reached a steady state situation. This means that the measured fluorescence within the time window of 20 seconds as indicated, may vary a few per cent when measured during the beginning of the time window or at the end.

Around the standard protocol we have carried out a number of numerical experiments to investigate the sensitivity of the amplification curve on:

- Anneal rate (decay enzymes 2%, decay rate capture probes 0%)
- The initial load of enzymes (decay rate activity enzymes 2%, decay rate capture probes 0%)
- Decay rate of capture probes (decay rate activity enzymes 2% per cycle)
- Dilution tests.

All results are shown either for the concentration of species A in the bulk (for qRT PCR results) or as the fraction of capture probes hybridized with targets out of the solution on a specific spot of the microarray (for RTA PCR results). The fraction of targets is a direct measure for the fluorescence measured.

Figure 7 shows the effect of a change in anneal rate constant k. Without going into detail the salt concentration is an important parameter and must be chosen carefully such that the bulk PCR process runs optimally while at the same time the conditions for hybridisation are well tuned (**Wetmur and Davidson, 1968; Sambrook and Russell, 2001; product information Invitrogen, 2011**).

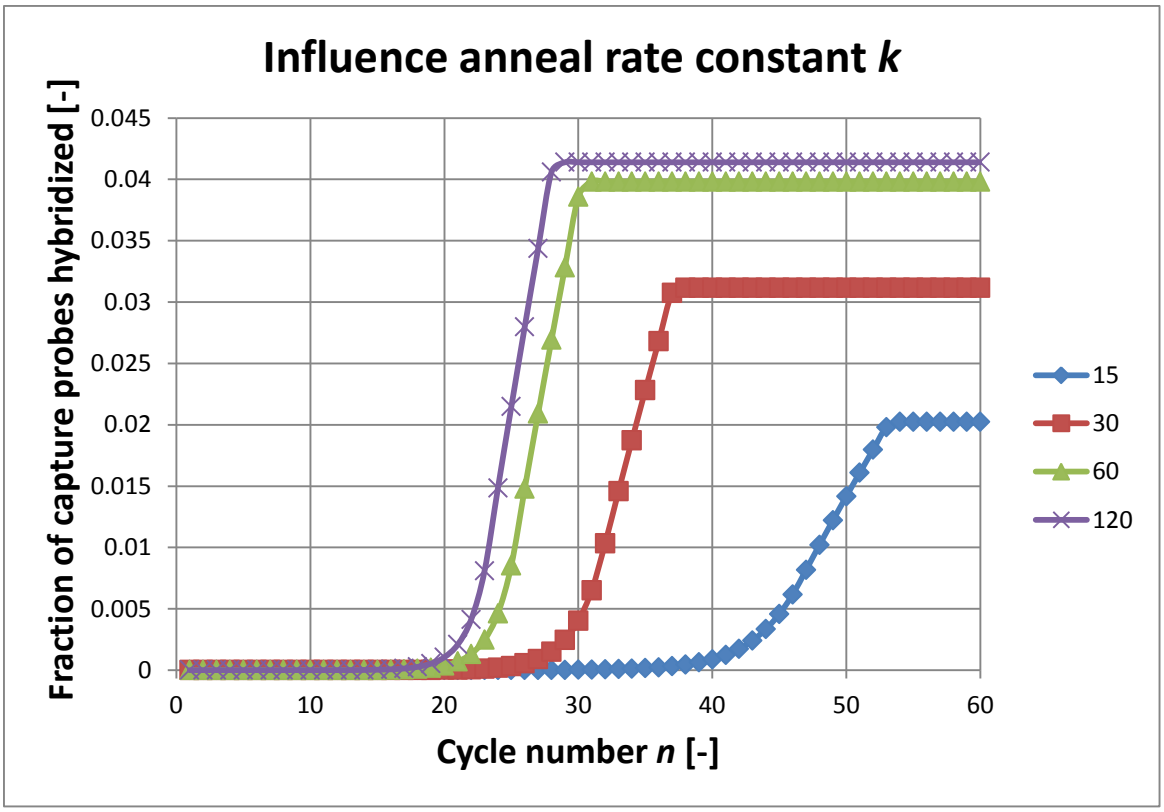

Figure 7 Influence of fraction of amplicons captured as a function of the anneal rate constant k. The anneal rate constant can very strongly depending on the salt concentration of the mix used. The values for k_{dsDNA} and k_{ass} are chosen relative to k ($k_{dsDNA} = k/2$, $k_{ass} = k/20$). For values of k higher than 120 m^3/mol/s there is no gain in amplification efficiency anymore.

During temperature cycling part of the polymerase will lose its activity (**Sambrook and Russell, 2001**). As explained earlier in paragraph 3.1 in this paper we will use 2% per cycle in our analysis following (**Whitney et al., 2004**).

As shown in figure 8 the effect of the reduction of the enzyme load may be considerable. The C_t value, however, is hardly dependent on the enzyme load at high and low input concentrations.

Not only enzymes may become inactive during cycling, the same may be true for the capture probes. The effect on the amplification curves is large as is displayed in figure 9. Remarkable, again, is that the effect is small on the C_t value.

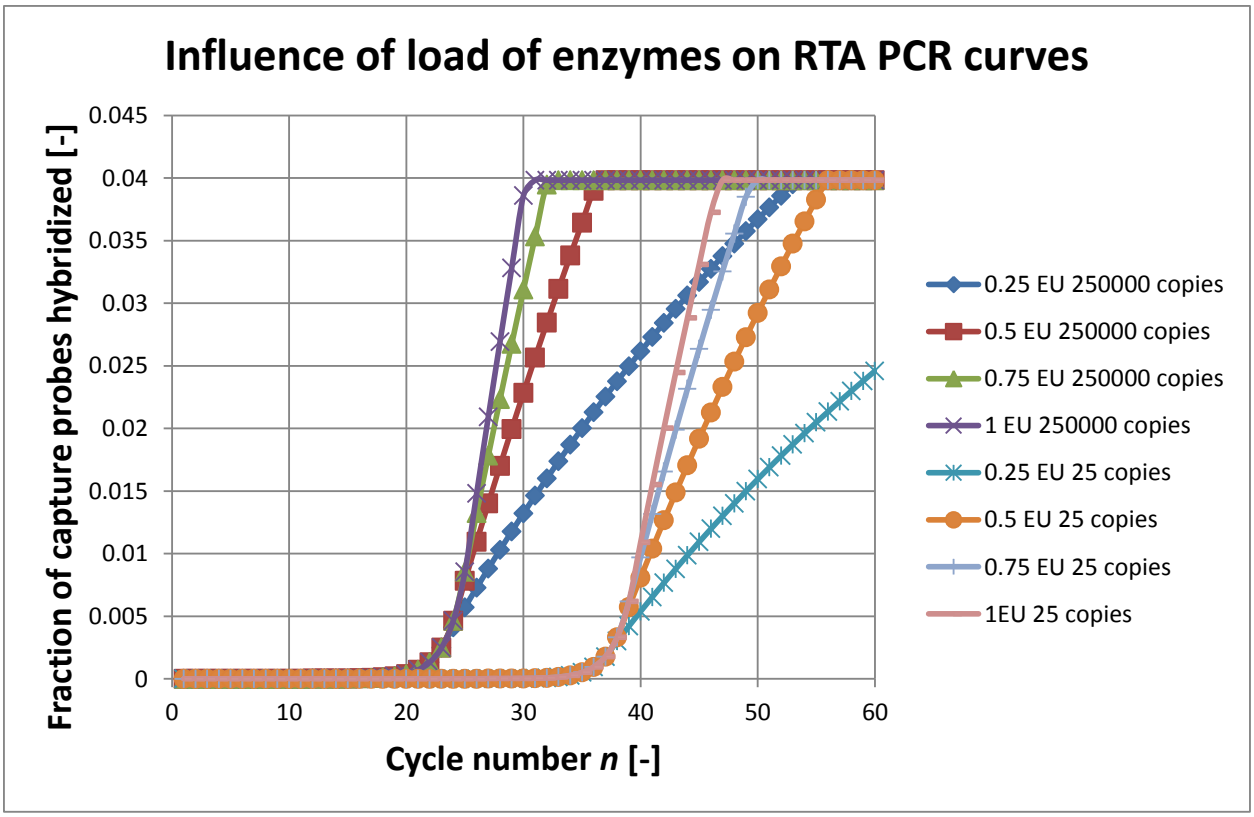

Figure 8 Influence of the initial enzyme load on the amplification curves presented as the fraction of capture probes immobilized on the array surface hybridized with targets out of the solution. The two sets of data indicate the behaviour for a high and a low expression of templates initially present in the bulk (see legend).

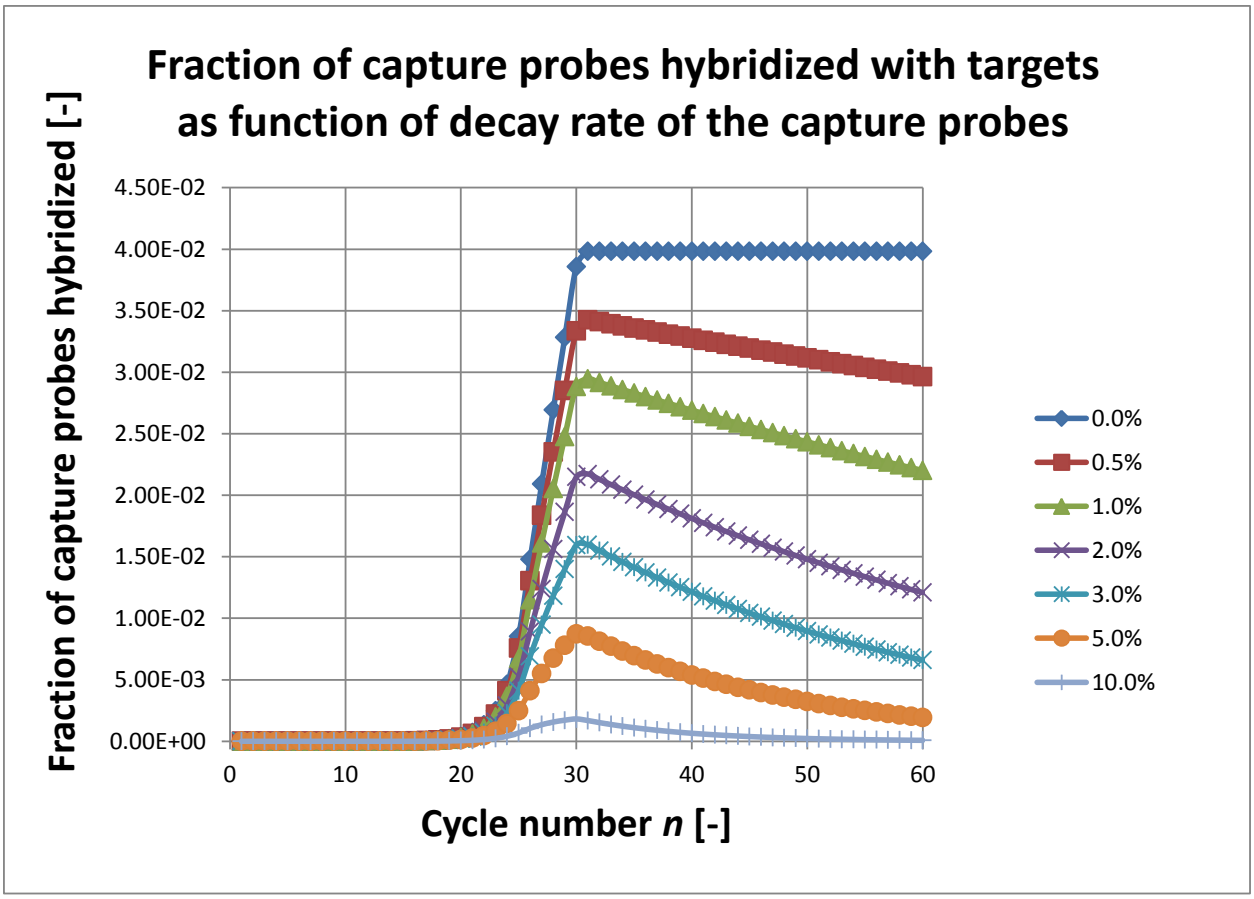

Figure 9 Dependence on the decay rate of the capture probe activity of the number of capture probes hybridized with targets out of the solution (given in fraction θ with respect to the initial situation) at the end of the annealing/hybridization step.

Our main result is about what happens when the initial expression of templates is reduced (dilution test). Here we have considered two cases, one with 0 % decay of activity of Taq per cycle and standard values for the annealing rate constants and another case with 2% decay of enzyme activity, 2% decay of capture probe activity and for which the annealing rate constants have been reduced. The results are displayed in figures 10 and 11.

The first case may be considered as representative for a standard qRT PCR process, because of the tight temperature control, highly temperature stable Taq and the use of plastic vials.
The second case may be close to the prototype RTA PCR process because of a change in salt concentration in order to optimize the surface hybridisation reaction and less stable temperature control. Together with surface absorption this causes a gradual decrease of enzyme activity. We also have taken into account that the salt concentration may not be optimally chosen, causing a significant reduction of the annealing rate constants in the bulk and at the surface. Unknown is the decrease in capture probe activity.

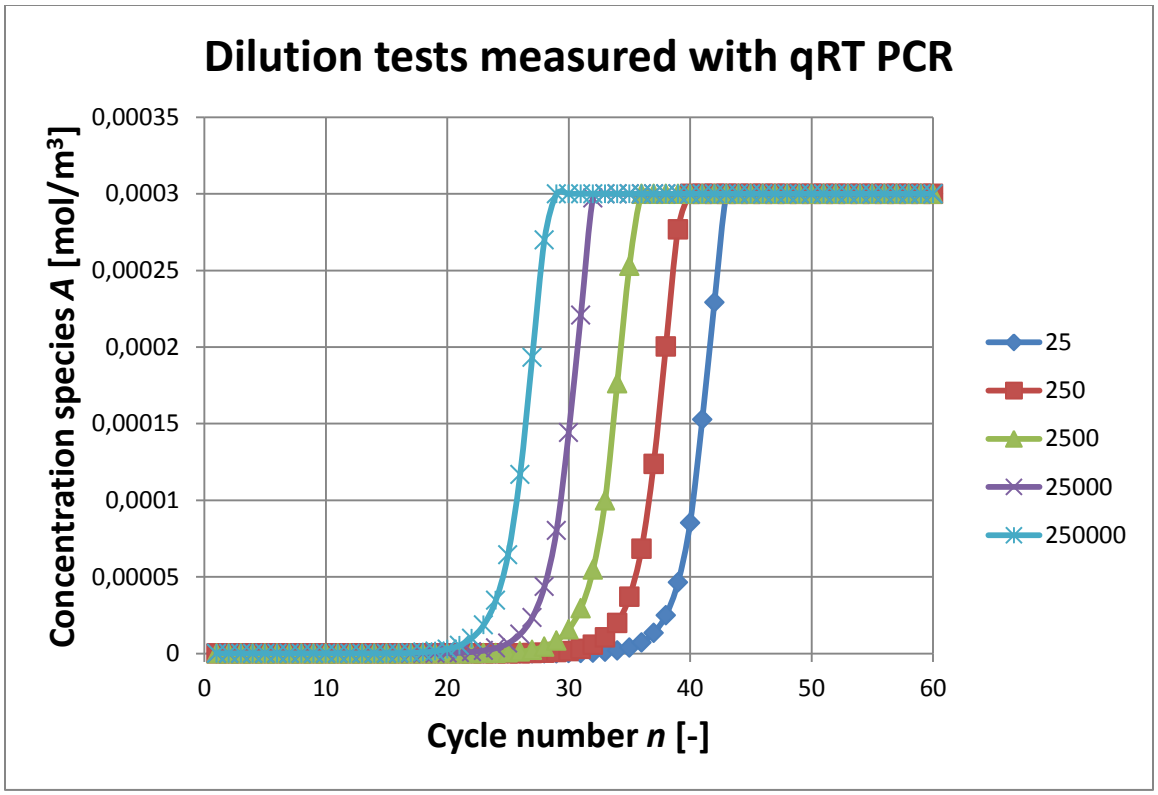

Figure 10 Results of a dilution test. The amplification curves hold for 0% decay of enzyme activity and the standard data for annealing and hybridisation. This case is considered representative for qRT PCR with precise temperature control, highly thermo-stable Taq and well-tuned salt concentration.

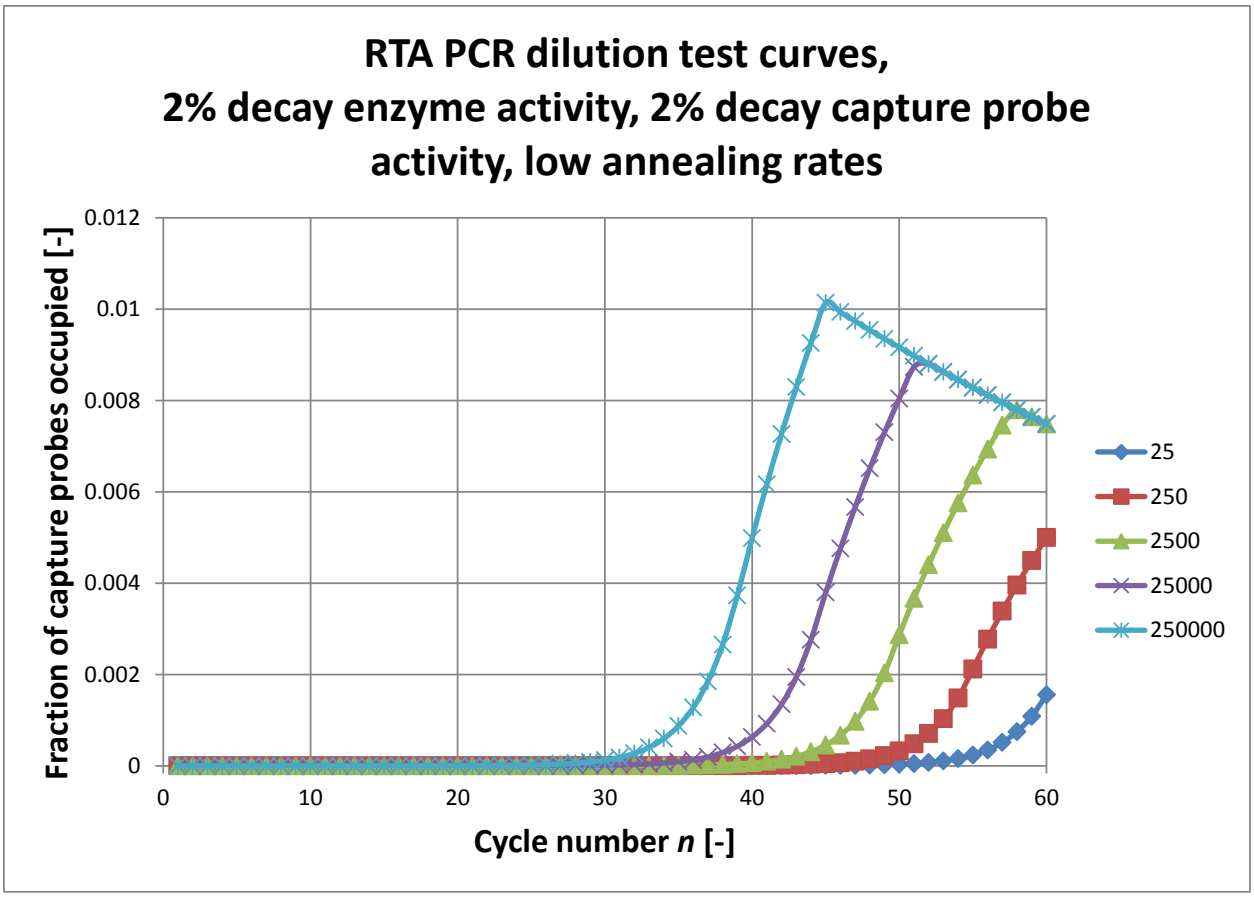

Figure 11 Influence of the initial template expression on the amplification curves as measured on the array surface. This case is considered to be representative for RTA PCR with a somewhat higher melting temperature in the PCR chamber due a less strict temperature control, adsorption of enzymes to the wall of the PCR chamber, fouling of capture probes and a slight change in salt concentration ($k = 20$ m^3/mol/s, $k_{dsDNA} = 10$ m^3/mol/s, $k = 1$ m^3/mol/s).

5 Conclusions

Real Time Array PCR is a novel biochemical technique to monitor the amplification reaction on a microarray surface and thereby determine the C_t values of a multiple of different templates in a PCR sample. It combines the quantitative measurement of real time process data as provided by the qPCR method and the high multiplex capability of a microarray based assay.

The collection of targets at the array surface scales with the concentration of labelled species at the beginning of the anneal process. At the end of the anneal process the concentration of labelled free targets approaches zero, stopping the hybridization reaction. From a detection point of view the RTA PCR process and the qRT PCR process deliver similar results. In a qRT PCR process using probes that open or are digested upon elongation, the bulk fluorescence is detected and recorded as amplification curve during thermal cycling. For the RTA PCR process labelled amplicons hybridize on a spotted microarray surface and the surface fluorescence is measured. Due to hybridization of targets on the microarray surface some unbalance between sense and antisense strands occurs in a small region above the microarray surface. This effect is small and our main conclusion is that the surface fluorescence scales with the bulk concentration.
The timing of the RTA PCR process is such that annealing of binary complexes and the formation of tertiary complexes is almost complete. According to our analysis, during the main part of thermal cycling elongation, at least up to the C_t value, elongation is 100%. We also see that elongation takes place during the annealing phase, this also causes that the elongation process nearly always ends up with full elongation. This is also true for the hybridization process. When only free single stranded DNA is able to hybridize on the microarray surface the hybridization reaction follows the timing of the annealing process and reaches almost the steady state value as well.

Our analysis shows that the C_t value is only slightly dependent on the initial enzyme load and the degradation of the capture probes. The C_t value, however, does depend strongly on the rate constants of the annealing/hybridization reactions in the bulk and on surface.

A main concern is the fouling of capture probes. When capture probes lose in course of the PCR process their ability to bind targets out of the solution, the sensitivity of the array based method decreases, especially for low expressions.

Acknowledgements

We acknowledge Reinhold Wimberger-Friedl for critically reviewing the manuscript.

References

Abramowitz, M., Stegun,I.A., 1970. Handbook of Mathematical Functions, 7-th Edition. Dover Publications.

Anderson, M.L.M., 1999. Nucleic Acid Hybridization. Bios Scientific Publishers.

Bird, R.B., Stewart, W.E., Lightfoot, E.N., 2002. Transport Phenomena, Second Edition, John Wiley & Sons.

Booth, C.S., Pienaar, E., Termaat, J.R., Whitney, S.E., Louw, T.M., Viljoen, H.J., 2010. Efficiency of the polymerase chain reaction. Chemical Engineering and Science 65, 4996-5006.

Carslaw, H.S., Jaeger, J.C., 1959. Conduction of Heat in Solids", Oxford at the Clarendon Press.

Dijksman, J.F., Pierik, A., 2008. Fluid dynamical analysis of the distribution of ink jet printed biomolecules in microarray substrates for genotyping applications. Biomicrofluidics 2: 044101 – 044122.

Erill, I., Campoy, S., Erill, N., Barbe, J., Aguilo, J., 2003. Biochemical analysis and optimization of inhibition and adsorption phenomena in glass-silicon PCR chips. Sensors and Actuators B 96, 685-692.

Fiche, J.B., Buhot, A., Calemczuk, R., Livache, T, 2007. Temperature Effects on DNA Chip Experiments from Surface Plasmon Resonance Imaging: Isotherms and Melting Curves. Biophys J 92, 935-946.

Gao, Y., Wolf, L.K., Georgiadis, R.M., 2006. Secondary structure effects on DNA hybridization kinetics. Nucleic Acids Research Vol 34, No 11, 3370-3377.

Gevertz, J.L., Dunn, S.M., Roth, C.M., 2005. Mathematical Model of Real-Time PCR Kinetics. Biotechnology and Bioengineering, DOI: 10.1002/bit.20617: 1- 10.

James G. Wetmur, J.G., Davidson, N., 1968. Kinetics of renaturation of DNA. J. Mol. Biol. 31, 349-370.

Khodakov, D.A., Zakharova, N.V., Gryadunov, D.A., Filatov, F.P., Zasedatelev, A.S., Mikhailovich V.M., 2008. An oligonucleotide microarray for multiplex real-time PCR identification of HIV-1, HBV, and HCV. Biotechniques 44, 241-248.

Landgraf, A., Wolfs, H., 1993. Taq Polymerase (E.C. 2.7.7.7) with Particular Emphasis on Its Use in PCR Protocols, in: Burrell, M.H. (Ed), Enzymes of Molecular Biology, Methods in Molecular Biology 16, chapter 4.

Mocanu, D., Kolesnychenko, A., Aarts, S., De Jong, A.T., Pierik, A., Coene, W., Vossenaar, E., Stapert, H., 2008. Quantitative analysis of DNA hybridization in a flow-through microarray for molecular testing. Analytical Biochemistry, doi: 10.1016/j.ab.2008.05.034.

Mocanu, M., Kolesnychenko, A., Aarts, S., De Jong, A.T., Pierik, A., Coene, W., Vossenaar, E., Stapert, H., 2009. Mass transfer effects on DNA hybridization in a flow through microarray. Journal of Biotechnology, doi: 10.1016/j.biotec.2008.10.001 .

Pappaert, K., Van Hummelen, P., Vanderhoeven, J., Baron, G.V., Desmet, G., 2003. Diffusion-reaction modelling of DNA hybridization kinetics on biochips. Chemical Engineering Science 58, 4921-4930.

Pierik, A., Dijksman, J.F., Raaijmakers, A., Wismans, A.J.J., Stapert, H.R., 2008. Quality control of inkjet technology for DNA microarray fabrication, Biotechnol J 3,1581-1590.

Pierik, A., Boamfa, M., Van Zelst, M., Clout, D., Stapert, H., Dijksman, J.F., Broer, D., Wimberger-Friedl, R., 2011. Real time quantitative amplification detection on a microarray: towards high multiplex quantitative PCR. Submitted for publication in Lab on a Chip.
Potrich, C., Lunelli, L., Forti, S., Vozzi, D., Pasquardini, L., Vanzetti, L., Panciatichi, C., Anderle, M., Pederzolli, C., 2010. Effect of materials for micro-electro-mechanical systems on PCR yield. Eur Biophys J 39: 979-986.
Reinick, P., Wienken, C.J., Braun, D., 2010, Thermophoresis of single stranded DNA. Electrophoresis, 31, 279-286.
Remacle, J., Alexandre, I., Margaine, S., Husar, D., 2006. Real-time quantification of multiple targets on a micro-array. Eppendorf Array Technologies patent EP1659183
Remacle, J., Alexandre, I., Koehn, H., Seippel, M., 2007. Lid for PCR vessel comprising probes permitting PCR amplification and detection of the PCR product by hybridisation without opening the PCR vessel, Eppendorf Array Technologies patent EP1788095.
Sambrook J., Russell, D.W., 2001. Molecular Cloning, Third Edition. Cold Spring Harbor Laboratory Press.
Schnell, S., Mendoza, C., 2000. Time-dependent Closed Form Solutions for Fully Competitive Enzyme Reactions. Bulletin of Mathematical Biology 62, 321-336.
Sprangler, R., Goddard, N.L., Thaler, D.S., 2009. Optimizing Taq Polymerase Concentration for Improved Signal-to-Noise Ratio in the Broad Range Detection of Low Abundance Bacteria, PlosOne, Volume 4, Issue 9, 1-9.
Squires, T.M., Messinger, R.J., Manalis, S.R., 2008. Making it stick: convection, reaction and diffusion in surface-based biosensors. Nature Biotechnology, Volume 26, Number 4, 417-426.
Szabo, I., 1959. Hütte, Mathematische Formeln und Tafeln. Verlag von Wilhelm Ernst & Sohn, Berlin.
Truskey, G.A., Yuan, F., Katz, D.F., 2010. Transport Phenomena in Biological Systems, Second Edition. Pearson Prentice Hall Bioengineering.
Wang, J.-Y., Drlica, K., 2003. Modeling hybridization kinetics. Mathematical Biosciences 183, 37–47.
Whitney, S.E., Sudhir, A., Nelson, R.M, Viljoen, H.J., 2004. Principles of rapid polymerase chain reactions: mathematical modeling and experimental verification. Computational Biology and Chemistry 28, 195-209.
www.invitrogen.com